Theor Chim Acta (1995) 92: 107–122

Theoretica Chimica Acta

Investigating optimal coordinates for describing vibrational motion

Rudolph C. Mayrhofer, Edwin L. Sibert III

Department of Chemistry and Theoretical Chemistry Institute, University of Wisconsin–Madison, Madison, WI 53706, USA

Received August 24, 1994/Final revision received December 18, 1994/Accepted December 18, 1994

Summary. Results of independent mode models of molecular vibrations of SO_2 and H_2O are compared to converged eigenvalues and eigenfunctions. Energies of self-consistent-field and adiabatic wave functions are calculated and compared to the eigenvalues; Brueckner functions and natural modals are compared to the eigenfunctions. These comparisons are made for a class of normal coordinates of varying curvature. Of the coordinates we considered, an independent mode model based on rectilinear normal coordinates provides the best description of the energetics yet provides the poorest description of the eigenfunctions. The ramifications of this finding are discussed for both independent mode models and perturbative descriptions of molecular vibrations.

Key words: Independent mode models – Vibrational coordinates – Perturbation theory

1. Introduction

A central goal of theoretical chemistry is to understand the connection between a Born–Oppenheimer potential energy surface and the dynamics that occurs on this surface. An important step in trying to understand this connection is the calculation of a rotation–vibration spectrum for the given potential energy surface. A large amount of research has been directed towards developing algorithms for rapid and accurate calculations of such spectra [1–7]. Implicit in each algorithm is a set of coordinates used to describe the vibrational motion. The choice of coordinates is crucial, since a judicious selection can significantly reduce the effort needed to solve for the vibrational eigenvalues and eigenfunctions. However, the coordinates should also provide some physical insight, as this aids in the interpretation of the results in light of some physical model. A related consideration in choosing the coordinates is to select a representation that minimizes the couplings amongst all the degrees of freedom.

In consideration of the above criteria, normal coordinates are a commonly used representation for describing molecular motion. In this representation, there are no

couplings through quadratic terms in the Hamiltonian. Therefore, low-lying states can be accurately written as a single product wave functions,

$$\Psi_n(\boldsymbol{Q}) = \prod_{i=1} \Phi_{n_i}(Q_i), \tag{1}$$

where Φ_{n_i} are harmonic oscillator functions and Q_i are the normal coordinates. This particular independent particle (or mode) model, has played a profound role in both interpretations and calculations of molecular properties. At higher levels of excitation, the exact wave function can no longer be expressed in this simple product form. Nonetheless, given a more judicious choice of both coordinates $\boldsymbol{Q}$ and functions Φ_{n_i}, a single product form of the wave function can provide a surprisingly accurate representation for determining a variety of molecular properties. In this paper we will examine several criteria for determining both these functions and coordinates.

Several groups have used the SCF energy as a criterion for optimizing a particular class of coordinates. Thompson and Truhlar have considered a rotation of the normal coordinates in order to optimize separability via the variational rotation angle [8]. Moiseyev showed that even though the variational determination of the rotation angles can be difficult, some values of the angle may be restricted based on physical arguments [9]. Bačić et al. developed a similar treatment for curvilinear motion of HCN. They variationally found the optimal coordinates among a class of spheroidal coordinates for describing isomerization motion [10]. Zúñiga et al. [11] considered a class of Jacobi coordinates using SCF energies to find the optimal member of that class for HCN. Gibson et al. used hyperspherical coordinates in a semiclassical SCF framework, and found them to be particularly effective for describing the highly excited vibrational states of H_2O and CO_2 [12]. Roth et al. applied the SCF method to compare normal modes and local modes [13]. They found that the local modes gave a better description of the energy for H_2O and CO_2 than do the normal modes.

Another criterion for judging the quality of independent particle models is the best density criterion. Here, natural modals have been used to analyze vibration–rotation wave functions of van der Waals systems [14], to study mode specificity in the localization of energy [15], to examine strongly coupled Morse oscillators [16], to classify vibrational states as ergodic [17], and to analyze separability of vibrational wave functions as a function of the curvature of the coordinate system [18]. In related work, Fleming and Hutchinson, have examined a class of coordinates defined as linear combinations of bond modes. The optimal coordinate rotation was defined as that which maximizes the projection of the exact wave function onto a particular zero-order state [19].

The above work has demonstrated that coordinate choice is an important component of independent mode models. In this paper we follow this lead and examine a class of normal coordinates introduced by Colbert and Sibert [18]. These coordinates are called the variable curvature coordinates (VCC), because the coordinate system is parametrized by a curvature variable which allows one to continuously vary the curvature of the coordinate system. Furthermore, we will apply the above-mentioned criteria for judging the quality of the independent mode model to show that different criteria lead to very different sets of optimal coordinates.

To illustrate these ideas, wave functions and energies for two nonlinear symmetric triatomics, SO_2 and H_2O are calculated using the VCC, in order to

determine the coordinate system that optimizes the independent mode model. If either the SCF energy or the adiabatic energy are used as a criterion to optimize the coordinates, we find that rectilinear normal coordinates give the *best* representation for the product function. However, when either the best density or best overlap criterion is used, we find that rectilinear normal coordinates give the *poorest* description. The optimal coordinates, determined via this criterion, have a curvature that is greater than that of the bond-angle representation.

In addition to the above independent particle models, we consider results of Van Vleck perturbation theory. McCoy and Sibert have examined the convergence of perturbation expansions of the energy and compared the results for vibrational Hamiltonians expressed as functions of curvilinear and rectilinear normal coordinates [25]. In this paper we discuss how perturbative results vary as a function of coordinate curvature.

The outline of this paper is as follows. In Sect. 2, we review the definition of the VCC and the techniques we use to variationally determine the molecular eigenfunctions in the VCC representation. We describe the criteria for judging the independent mode model and present the results of these criteria as a function of coordinate curvature in Sect. 3. The sensitivity of perturbative expansions to the coordinate curvature are presented and discussed in Sect. 4. The results of this study are summarized in Sect. 5.

2. The variable curvature coordinates

Colbert and Sibert have defined the VCC for several model problems as well as for nonlinear triatomic molecules [18]. For ABA triatomic molecules, the coordinates are parametrized by a single variable l which controls the curvature associated with the extension of the bend coordinate for fixed values of the two stretch coordinates. One well-known limit of this class of coordinates is the internal bond-angle extension coordinates ($l = 0$). The member for $l = \infty$ is the rectilinear internal coordinates used by Wilson et al. [26]. These coordinates, which are linear combinations of the Cartesian coordinates, are identical to the bond-angle extension coordinates in the limit of small amplitude motion. The molecules in Fig. 1 correspond to extension of the bend, with fixed stretch extensions. The top figure corresponds to a coordinate system where the bend motion is characterized by a curvature greater ($l < 0$) than that of the bond-angle coordinates. Optimizing coordinates by varying the curvature has also been recently studied by Bastida et al. [27], who considered a class of hyperspherical coordinates to investigate nonbending models of H_2O and CO_2.

Previous work has shown that the separability of the wave function is sensitive to the choice of the linear combination of internal coordinates [28] and that the transformation that leads to the *normal* coordinates often gives the lowest SCF vibrational energies. Therefore, we use the linear combination of VCC that give rise to normal coordinates. We label the normal coordinates according to the standard spectroscopic convention where Q_1 and Q_3 are the symmetric and asymmetric stretch coordinates, respectively, and Q_2 is the bend coordinate. The normal mode VCC are linearly related to the VCC internal coordinates via the linear transformation

$$\boldsymbol{Q} = \boldsymbol{L}^{-1}\boldsymbol{S}. \tag{2}$$

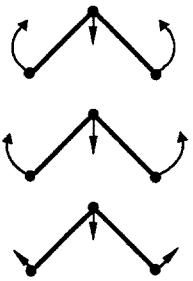

Fig. 1. Vibrational motion of the nuclei for different values of the curvature. The top plot corresponds to ($l < 0$), the middle plot is the bond-angle limit ($l = 0$) and the bottom plot is the rectilinear limit of the VCC($l \to \infty$). In the limit of small amplitude motion, all these motions are identical

Here $\boldsymbol{L}$ is the standard matrix used by Wilson et al. [26]; this matrix is not a function of the curvature. Since the VCC internal coordinates are identical to bond-angle coordinates in the limit of small amplitude motion, the quadratic contributions to the Hamiltonian are invariant to the curvature of the coordinate system.

We now turn to discussion of the methods we have implemented to obtain the vibrational eigenfunctions and eigenvalues. Our approach is general, since it requires finding the eigenvalues and eigenfunctions of a class of coordinates and therefore a class of Hamiltonians.

The most general form of the $J = 0$ vibrational Hamiltonian for a nonlinear polyatomic molecule is

$$\hat{H} = \frac{1}{2}\sum_{ij} \hat{P}_i G_{ij}(\boldsymbol{Q}) \hat{P}_j + V'(\boldsymbol{Q}) + V(\boldsymbol{Q}), \tag{3}$$

where G_{ij} are the G matrix elements given by Wilson et al. [26]. $V'(\boldsymbol{Q})$ is typically small and arises from the transformation of the kinetic energy operator from Cartesian coordinates to curvilinear internal coordinates. The volume element for the Hamiltonian in Eq. (3) is $\mathrm{d}\boldsymbol{Q} = \mathrm{d}Q_1\,\mathrm{d}Q_2\,\mathrm{d}Q_3$. The form for the above Hamiltonian operator is general; it therefore applies for the VCC. The $\boldsymbol{G}$ matrix elements can be written as functions of the atomic masses and the $\boldsymbol{B}$ matrix as [26]

$$G_{ij} = \sum_k B_{ik} m_k^{-1} B_{jk}, \tag{4}$$

where the elements of the matrix $\boldsymbol{B}$ are defined

$$B_{ik} = \frac{\partial Q_i}{\partial x_k} = \sum_l L_{il}^{-1} \frac{\partial S_l}{\partial x_k}, \tag{5}$$

Here Q_i are the normal mode VCC, S_l are the internal VCC, and x_k are the Cartesian displacement coordinates. In our work the derivatives in this equation are calculated analytically [18]. The form of $V'(\boldsymbol{Q})$ is more complicated, so we expanded this term numerically in a Taylor series to fourth order around the equilibrium position in terms of the VCC.

The potential energy surface we used for SO_2 is expressed as a function of the bond-angle internal coordinates [29]. The force field we used for H_2O was

constructed by Halonen and Carrington [30]. Their potential is expressed as a quartic expansion in terms of the bend extensions and Morse variables $y_i = D_e[1 - \exp(-\alpha r_i)]$ where r_i is a bond extension coordinate. Following the ideas of Carter and Handy, we modified the H_2O surface slightly so the barrier to linear configuration has the correct boundary conditions, i.e. $\partial V/\partial\theta|_{\theta=\pi} = 0$ [31].

An important consideration in our choice of basis set is that it be flexible enough to describe the continuous changes in the coordinate system. We have found that a distributed Gaussian basis (DGB) set provides this flexibility. This basis has been used to calculate effectively vibrational energies and wave functions [6, 32, 33]. The form for these basis functions is

$$\chi_{n_i}(Q_i) = \left(\frac{2A^{(Q_i)}}{\pi}\right)^{1/4} \exp[-A^{(Q_i)}(Q_i - Q_{in})^2]. \tag{6}$$

In Eq. (6), Q_{in} define the center of the Gaussian χ_{n_i} for the ith degree of freedom. The centers are equally spaced over the potential surface along each degree of freedom. For each degree of freedom, the Gaussians have a constant width $A^{(Q_i)} = A_i$. The three values for these widths are optimized by minimizing the vibrational energies for two two-dimensional Hamiltonians. First A_1 and A_2 are determined by setting $Q_3 = 0$ and minimizing the two-dimensional symmetric stretch–bend energies as a function of A_1 nd A_2. Then A_3 is determined by setting $Q_1 = 0$ and minimizing the asymmetric stretch–bend energies with respect to A_3. These minimizations of A_i, carried out once for $l = 0$, are not repeated for other values of the curvature.

To calculate the kinetic and potential energy matrix elements, an evenly spaced three-dimensional grid of points for the normal mode VCC is selected. These matrix elements are calculated by Gauss–Hermite quadrature using 4 points in each degree of freedom. Both the Hamiltonian and overlap matrices are constructed using symmetrized wave functions which reflect the C_{2v} symmetry of nonlinear symmetric triatomics. The generalized eigenvalue equation, $\boldsymbol{H} - \boldsymbol{ES} = 0$, is solved. For H_2O, 8 Gaussians were placed along each stretch, and 12 Gaussians were placed along the bend to give a total of 768 functions. After symmetrization, the symmetric matrix contained 432 functions and antisymmetric matrix contained 336 functions. Variationally converged energies for SO_2 and H_2O (to within 0.2 cm^{-1}) are presented in Tables 1 and 2, respectively.

As a word of caution, we note that using normal coordinates and the associated volume elements leads to a Hamiltonian with singularities in V' at the linear configuration of the molecule. For this reason, the Gaussian basis sets are not useful for describing the highly excited bend states of H_2O. This shortcoming holds true for all normal mode Hamiltonians.

3. Independent mode models

In this section the vibrational energies and wave functions Φ_{n_i} of SO_2 and H_2O are analyzed using the criteria suggested by Kutzelnigg and Smith [20]. In contrast to our work, their study characterized independent particle models for electronic structure wave functions. In the following paragraphs we review these standards along with an adiabatic calculation of the vibrational energies. We then determine optimal coordinates for a single product expansion of the vibrational wave function for each of the criteria.

Table 1. Vibrational energies for SO_2 in units of cm^{-1} where $l = 0$ Å

State	Variational	SCF[a]	Density modal[a]	Adiabatic[a]
0, 0, 0	1526.6	1.6	1.6	0.0
0, 1, 0	2042.0	2.0	2.0	0.2
0, 2, 0	2553.0	3.5	3.6	1.6
1, 0, 0	2677.9	6.2	6.4	− 0.9
0, 0, 1	2889.0	4.7	4.7	0.0
0, 3, 0	3059.9	5.9	5.9	3.9
1, 1, 0	3193.9	5.4	5.7	− 2.4
0, 1, 1	3403.8	5.2	5.3	0.3
0, 4, 0	3562.6	9.0	9.1	7.1
1, 2, 0	3705.2	6.2	6.4	− 2.3
1, 3, 0	4212.0	8.1	8.2	− 1.0
2, 2, 0	4850.2	8.9	9.8	− 6.3
1, 2, 1	5052.4	20.0	20.8	− 2.3
2, 0, 1	5156.0	35.2	37.6	− 1.9
0, 2, 2	5264.6	7.9	7.9	2.3
2, 3, 0	5356.9	10.4	11.5	− 6.0
1, 0, 2	5364.0	30.7	32.2	− 0.2
3, 1, 0	5476.8	12.0	13.8	− 7.9
1, 3, 1	5558.5	22.2	23.1	− 0.8
0, 0, 3	5581.8	3.4	3.4	4.1
2, 1, 1	5672.2	33.0	35.7	− 5.3
0, 3, 2	5770.2	10.7	10.8	4.9
1, 1, 2	5879.0	29.9	31.4	− 1.8
3, 2, 0	5988.3	11.5	13.7	− 10.3
4, 0, 0	6095.3	16.4	19.1	− 6.8
2, 2, 1	6183.0	33.4	36.1	− 6.4

[a] Difference between approximate single configuration energies and exact energies. States with 5 or more quanta of excitation in the bend are not displayed, and only select states between 3800–5000 cm^{-1} are displayed

2.1. Wave function analysis

Brueckner orbitals [34] are defined to maximize the projection of a single configuration product basis onto the exact eigenfunction, and natural modals are defined to diagonalize the first-order density matrix. The natural orbital expansion was developed to examine electronic wave functions and to reduce the number of configurations in the expansion of the wave function [35]. The natural modals have also been used to examine vibrational wave functions, since very few configurations of the natural modals are needed to describe the exact wave function [36].

For SO_2 the wave functions are expanded as

$$\Psi_r(Q_1, Q_2, Q_3) = \sum_{l,m,n} \bar{C}^{(r)}_{lmn} F_l(Q_1) G_m(Q_2) H_n(Q_3), \tag{7}$$

where F_l, G_m and H_n are the natural modals. For H_2O, the wave functions are expanded in terms of natural modals and geminals,

$$\Psi_r(Q_1, Q_2, Q_3) = \sum_{nm} \bar{C}^{(r)}_{nm} F_n(Q_1, Q_3) G_m(Q_2), \tag{8}$$

Table 2. Select vibrational energies for H_2O in units of cm^{-1} where $l = 0$ Å

State[a]	Variational	SCF[b]	Density modal[b]	Adiabatic[b]
(0, 0) 0	4627.5	1.3	1.3	0.5
(0, 0) 1	6222.2	4.2	4.2	2.8
(0, 0) 2	7779.6	7.8	8.0	9.3
$(1, 0)^+$ 0	8284.5	2.3	2.4	− 1.2
$(1, 0)^-$ 0	8382.3	2.0	2.1	0.8
(0, 0) 3	9297.4	12.2	12.3	19.2
$(1, 0)^+$ 1	9860.1	9.0	9.2	− 1.9
$(1, 0)^-$ 1	9956.6	6.8	6.8	3.4
(0, 0) 4	10771.8	16.2	16.2	31.4
(1, 1) 2	15141.8	19.6	19.6	9.8
$(3, 0)^+$ 0	15249.8	2.3	2.7	− 6.1
$(3, 0)^-$ 0	15266.2	2.5	2.6	− 5.7
$(2, 1)^+$ 0	15503.7	3.4	3.4	− 0.8
$(2, 1)^-$ 0	15659.8	4.1	4.1	1.3
$(2, 0)^+$ 3	16379.6	40.2	40.3	8.3
$(2, 0)^-$ 3	16428.2	34.0	34.6	16.1
(1, 1) 3	16618.5	28.7	28.7	19.9
$(3, 0)^+$ 1	16782.9	16.7	17.2	− 2.6
$(3, 0)^-$ 1	16798.6	16.1	16.5	− 0.1
$(2, 1)^+$ 1	17038.7	17.8	18.2	− 0.7
$(2, 1)^-$ 1	17193.7	15.4	15.6	4.6
$(2, 1)^+$ 2	18543.8	23.9	24.1	− 5.4
$(2, 1)^-$ 2	18688.8	27.0	27.2	11.7

[a] The states are labeled using local mode notation

[b] Differences between approximatie energies and exact energies.

where the modal describes the bend degree of freedom and the geminal describes both stretch degrees of freedom. There is a strong 2:2 Darling–Dennison resonance between the two stretch modes. Consequently these two modes cannot be expressed using simple product functions. Furthermore, the mixing between the stretch modes in H_2O is insensitive to the curvature of the bending coordinate.

The full variational calculation is carried out at several values of the curvature, and the natural modals are then constructed for each state using standard methods. For H_2O we used the Carlson–Keller theorem [37] to simplify the expansion of Eq. (8) to

$$\Psi_r(Q_1, Q_2, Q_3) = \sum_n \bar{C}_n^{(r)} F_n(Q_1, Q_3) G_n(Q_2). \tag{9}$$

Here there are no cross terms in the expansion of the wave function, and the expansion coefficients are related to the eigenvalues Λ_n of the one-modal density matrix by the relation $\bar{C}_n^{(r)} = \Lambda_n^{1/2}$.

Löwdin and Shull have shown that natural orbitals and Brueckner orbitals are equivalent if only two orbitals F_n and G_n are used to describe the coordinates of interest [38]. For SO_2 we iteratively remove all singly excited expansion coefficients in Eq. (7) in order to find the Brueckner modals, i.e. best overlap wave function. To illustrate this iterative process we show a simple two-dimensional

example of a wave function expanded in an orthonormal basis set

$$\Psi_r(Q_1,Q_2) = c_{11}F_1(Q_1)G_1(Q_2) + c_{12}F_2(Q_1)G_1(Q_2) + c_{22}F_2(Q_1)G_2(Q_2), \quad (10)$$

where c_{11} is greater than the other two expansion coefficients. In order to find the Brueckner function we iteratively remove all the singly excited expansion coefficients, there being just the one c_{12} term in the present example, via the orthogonal transformation

$$F'_1 = [c_{11}F_1 + c_{12}F_2]/(c_{11}^2 + c_{12}^2)^{1/2},$$
$$F'_2 = [c_{11}F_2 - c_{12}F_1]/(c_{11}^2 + c_{12}^2)^{1/2}. \quad (11)$$

to obtain

$$\Psi_r(Q_1, Q_2) = d_{11}F'_1(Q_1)G_1(Q_2) + d_{12}F'_2(Q_1)G_1(Q_2) + d_{22}F'_2(Q_1)G_2(Q_2). \quad (12)$$

In this new representation the singly excited expansion coefficient is reduced in magnitude to be

$$d_{12} = c_{12}c_{22}/(c_{11}^2 + c_{12}^2)^{1/2}. \quad (13)$$

The natural orbitals were used as the first step in this process. Since a single configuration typically dominates the expansion, the iteration proceeds rapidly. Indeed, the Brueckner functions and the natural orbitals were found to be very similar for the systems we investigated, so in this paper we mainly present results for the Brueckner functions.

2.2. Self-consistent-field calculation

The SCF approach provides an alternative method for determining optimal product functions. For a thorough review of the research on applying the SCF method to calculating vibrational energies and wave functions see the papers by Gerber et al. [39] and Ratner et al. [28].

In contrast to the Brueckner orbitals, where the overlap of the product basis with respect to the exact wave function is maximized, the SCF modals are chosen such that the following functional is satisfied:

$$\delta \frac{\langle \Psi_n | \hat{H} | \Psi_n \rangle}{\langle \Psi_n | \Psi_n \rangle} = 0. \quad (14)$$

The functional is constructed by inserting a product wave function into Eq. (14); this leads directly to the standard set of integro-differential equations for the SCF modals. The modals can be determined iteratively using either propagation methods such as the Cooley–Numerov method [40] or they can be determined by expanding the modals in a basis and using matrix algebra to solve the differential equations [41]. We use the later method. The modals are expanded in the DGB's, and unitary transformations are applied to small subsets of the Hamiltonian until self-consistency is achieved for the energy.

The SCF wave functions have the same form as for the natural modal expansion. For SO_2 we expand in modals, and for H_2O we expand in terms of modals and geminals.

2.3. *Adiabatic calculation*

The adiabatic approximation takes advantage of a dynamic separability [22, 23, 42, 43]. The assumption here is that there is some widely separated time scale for the motion of the nuclei. This is a good approximation, since the stretch frequency is at least a factor of two larger than the bend frequency in both H_2O and SO_2. Despite the frequency disparity, the approximation will breakdown for H_2O at high energies where there are 5–6 quanta of OH stretch excitation and the 2:1 stretch–bend Fermi resonance effects become pronounced.

We follow a similar approach of constructing the adiabatic wave functions as Johnson and Reinhardt [22]. The key difference is that these workers used Radau coordinates. The vibrational adiabatic wave function is written as

$$\Psi^{\mathrm{ad}}_{mn}(Q_1, Q_2, Q_3) = \chi_m(Q_1, Q_3; Q_2)\phi^m_n(Q_2), \tag{15}$$

where the stretch function χ_m is parametrized by the bend coordinate. The stretch functions are eigenfunctions of

$$\hat{H}_s(Q_2) = \tfrac{1}{2}\hat{P}_1 G_{11}\hat{P}_1 + \tfrac{1}{2}\hat{P}_1 G_{13}\hat{P}_3 + \tfrac{1}{2}\hat{P}_3 G_{31}\hat{P}_1 + \tfrac{1}{2}\hat{P}_3 G_{33}\hat{P}_3 + V'(\boldsymbol{Q}) + V(\boldsymbol{Q}), \tag{16}$$

where $\hat{H}_s(Q_2)$ is a portion of the full Hamiltonian in Eq. (3). The corresponding eigenvalues $E_m(Q_2)$, are obtained variationally using a DGB basis set. The bend functions are eigenfunctions of

$$\hat{H}_b = \tfrac{1}{2}\hat{P}_2 G_m(Q_2)\hat{P}_2 + E_m(Q_2) + E_{\mathrm{dac}}(Q_2), \tag{17}$$

where E_{dac} contains the diagonal adiabatic corrections. These functions also were obtained variationally using a DGB basis.

2.4. *Discussion*

In this section we apply the above-discussed criteria to investigate the optimal coordinates as a function of the curvature of the coordinate system. Before doing so, however, we discuss a simple, visual criterion for gauging the optimal coordinates of vibrational wave functions as a function of coordinate curvature.

In Fig. 2 we have displayed an eigenfunction of SO_2 in three coordinate systems. If these wave functions could be expressed in the single-product form $\Psi_n(\boldsymbol{Q}) = \prod_{i=1} \Phi_{n_i}(Q_i)$, then the nodal pattern would look like a "checkerboard"; the nodal lines would intersect each other at right angles and exhibit no curvature. The nodal lines of the wave function in Fig. 2a have considerable curvature. This curvature is readily reduced in the VCC by decreasing the value of l, and thereby increasing the curvature of the coordinate system (cf. Fig. 2b, c).

We analyze separability as a function of curvature in a more quantitative manner by plotting the leading expansion coefficient of the Brueckner orbitals against the curvature of the coordinate system. The results for several wave functions are shown for SO_2 in Fig. 3. The magnitudes of the leading expansion coefficients are all monotonically decreasing functions that show maxima for $l < 0$. This behavior is similar to that found by Colbert and Sibert in an earlier study of two-dimensional model problems [18]. We also observe the same trends for H_2O.

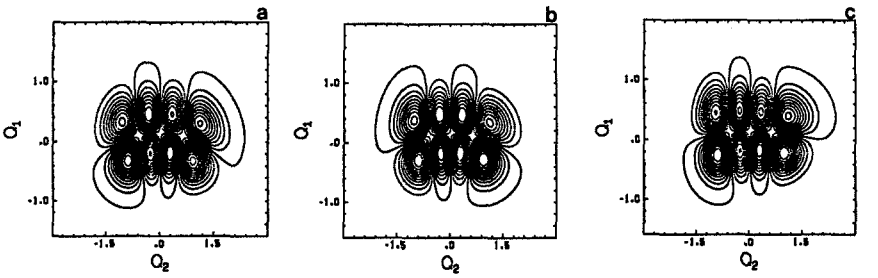

Fig. 2. $Q_3 = 0$ slices through the SO_2 vibrational wave function (1,3,0) for various values of the curvature. The values of l for the figures from top to bottom are 3.18, 0.0 and -0.79 Å. Notice as the curvature of the coordinates increases, the curvature in the nodal pattern of the wave function decreases

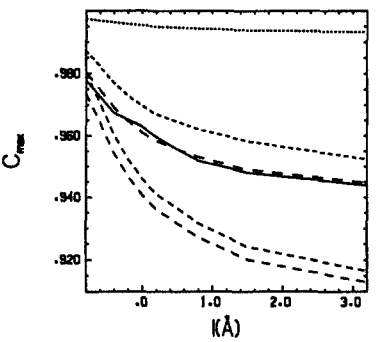

Fig. 3. The largest Brueckner expansion coefficient for SO_2 is plotted against l (cf. Fig. 2). The dashed curves are labeled from top to bottom as (0,2,0), (1,2,0), (1,3,0), (2,2,0) and (1,2,1). The solid curve is the average of the largest Brueckner coefficients for the 14 highest energy functions of Table 1

Although the $C_{max}(l)$ will certainly reach a maximum and then decrease as l is further decreased, we were unable to increase the curvature beyond the values given in the figure, as a result of numerical difficulties with the transformation from the VCC to the bond-angle coordinates.

Although the functional dependence of $C_{max}(l)$ varies from state to state, for example, the ground state expansion coefficient (cf. the uppermost curve) is an insensitive function of the curvature, as the total energy of the system is increased, anharmonic terms play an increased role, and the maximum expansion coefficients become more sensitive functions of the coordinate curvature. The important trend to note in this plot is that the wave functions can be represented best by a single-product configuration in the regime of small l over a large range of energies. These simple trends are expected to break down at higher energies where resonance interactions lead to substantially more complicated wave functions. At these higher energies, simply changing the curvature is not expected to significantly improve the separability of the wave functions. In fact, we have shown [18] in the case of CO_2 that, when there is a strong 2:1 stretch–bend Fermi resonance, $C_{max}(l)$ is an extremely insensitive function of the curvature of the coordinate system.

The SCF energy is plotted in Fig. 4 as a function of l. Based upon the previous results, one would expect the correlation energy to decrease as l is decreased. However, our plots show the *opposite* trend for the SCF calculation for most of the vibrational states below 6000 cm^{-1}. Thus, according to this criterion, the rectilinear limit provides the best independent particle model. Figures 3 and 4 constitute

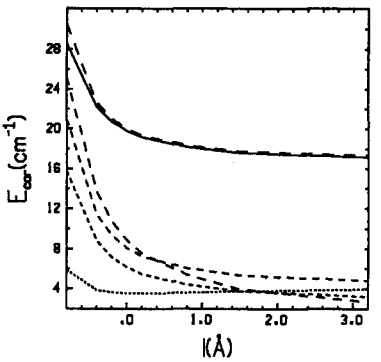

Fig. 4. The correlation energy for SO_2 is plotted against l. With the left side of the graph being the reference point, the dashed curves from top to bottom are labeled (1,2,1), (2,2,0), (1,3,0), (1,2,0) and (0,2,0). The solid curve is the average of the correlation energies for the 14 highest energy functions of Table 1

the two major points of this paper. First, the curvature parameter of the VCC provides a simple way of improving on the independent mode models. But, second, the optimal choice of l, i.e. the choice of coordinates is a very strong function of choice of criteria for evalutating the single-mode model.

The above result is unexpected. To check it, we calculated the energy of the natural modal associated with the largest coefficient and found that the natural modal energy was indeed larger than the SCF energy for every state. This result must hold, since the SCF orbitals are defined to give the best energy for a single-product basis. We also used the SCF functions in a full configuration-interaction (CI) calculation. The invariance of the resulting eigenvalues with respect to changes in the coordinate curvature provided us with an accurate check of our SCF results.

Certain and Moiseyev compared the adiabatic method with the SCF method to calculate highly excited vibrational states of two strongly coupled modes [43]. They found that the adiabatic calculation described the strongly coupled modes better than the SCF calculation. Both methods are similar in that there is some separability in the modes but there is a distinction in the way they assume the separability. The nodal patterns of an adiabatic wave function need not have the same "checkerboard" pattern found for the SCF wave functions. We have therefore included in our investigation a plot of the differences between adiabatic energies and exact energies of SO_2 against the curvature in Fig. 5. We find the same trends as were reported above for the SCF calculation. However, in contrast to the SCF results, the adiabatic energies often fall below the variational energies.

4. Perturbation theory

In the proceeding sections, our study focused on quantifying the accuracy of independent mode models as a function of coordinate curvature. Part of the importance of this study stems from the fact that, as chemists, we often use independent mode models as a way to gain insight into complicated molecular systems where no exact analytical solutions are available. Normal modes play just such a role in the interpretation of spectra associated with low levels of vibrational excitation. We have shown above, however that one can construct an entire class of normal coordinates of varying curvature. Furthermore, the extent of mixing between normal modes, depends both on the particular choice of normal modes and on the criterion used to measure the breakdown of the independent mode

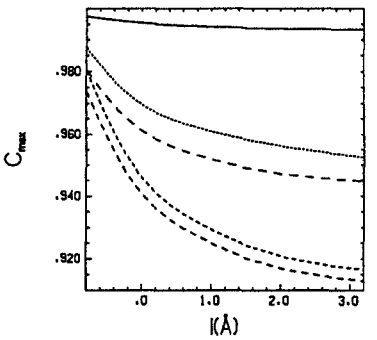

Fig. 5. The difference between the adiabatic energy and the variationally exact energy for SO_2 is plotted against I. The curves are labeled from top to bottom as (0,2,0), (1,3,0), (1,2,0), (1,2,1) and (2,2,0)

model. In this section, we discuss, some of the ramifications of the multiple normal mode descriptions as they apply to perturbation theory.

Except for recent work based on local mode perspectives [44–46], the preponderance of perturbative analyses have been developed as extensions to the rectilinear normal mode picture [47–49]. Recently, McCoy and Sibert compared rectilinear and curvilinear normal mode descriptions of three linear molecules, CO_2, HCN, and HCCH [25]. Here the curvilinear normal coordinates are defined as those which are obtained by taking the appropriate linear combination of the bond-angle coordinates, such that the Hamiltonian is separable through quadratic terms. These workers found for CO_2 that the perturbative expansion of the energy levels converged faster for the curvilinear representation. In contrast, for HCN the perturbative expansions are equivalent in these two representations.

In the absence of significant resonance interactions, the Hamiltonian derived from second-order perturbation theory is

$$\hat{H} = \sum_i \omega_i(\hat{n}_i + \tfrac{1}{2}) + \sum_{i \geq j} \chi_{ij}(\hat{n}_i + \tfrac{1}{2})(\hat{n}_j + \tfrac{1}{2}), \tag{18}$$

where $\hat{n}_i \equiv a_i^\dagger a_i$ is the number operator for the ith normal mode. The zeroth-order contribution to $\hat{H}$ consists of three uncoupled harmonic oscillators; the second-order terms are anharmonic correction terms. As originally developed, this expression was obtained from perturbative analysis based on rectilinear normal coordinates, and the above anharmonic correction terms are known functions of the parameters used to describe the potential energy surface. In fact, however, the numerical values of the anharmonic correction terms are invariant to the curvature of the normal coordinates [25].

In the more general case, where there are some important couplings between the molecular vibrations, a more complicated expression is needed to describe the energy levels. For example, Benedict et al. [50] showed that perturbation theory could be used to transform the full vibrational Hamiltonian to the block-diagonal form

$$\hat{H} = \sum_i \omega_i(\hat{n}_i + \tfrac{1}{2}) + \sum_{i \geq j} \chi_{ij}(\hat{n}_i + \tfrac{1}{2})(\hat{n}_j + \tfrac{1}{2})$$

$$+ \frac{k_{122}}{8^{1/2}}(a_1^\dagger a_2 a_2 + a_1 a_2^\dagger a_2^\dagger) + \frac{k_{1133}}{4}(a_1^\dagger a_1^\dagger a_3 a_3 + a_1 a_1 a_3^\dagger a_3^\dagger). \tag{19}$$

Table 3. Spectroscopic constants for SO_2 at various curvature values

Term	Rectilinear	Internal	Hypercurvature[a]
ω_1	1164.70	1164.70	1164.70
ω_2	519.52	519.52	519.52
ω_3	1380.37	1380.37	1380.37
χ_{11}	− 3.364	− 3.364	− 3.414
χ_{22}	− 1.226	− 1.160	− 1.670
χ_{33}	− 5.437	− 5.437	− 5.245
χ_{12}	− 2.648	− 1.114	− 0.743
χ_{13}	− 13.80	− 13.80	− 13.77
χ_{23}	− 0.525	− 0.525	− 0.574
$\lvert k_{122}\rvert$	30.59	23.48	22.92
k_{1133}	− 16.94	− 16.80	− 16.74

[a] $l = -0.25$ Å

This Hamiltonian, expressed as a function of number operators and off-diagonal creation and annihilation operators, is the same as that Eq. (18) with the exception of two terms that couple specific sets of states. The off-diagonal coupling term, proportional to k_{122}, allows for the 2:1 Fermi resonance interaction between the symmetric stretch and bend. The term proportional to k_{1133}, allows for the 2:2 Darling–Dennison resonance coupling between the symmetric and asymmetric stretches. Due to off-diagonal coupling terms the numerical values of the coefficients in this Hamiltonian are dependent on the choice of the coordinate curvature [25]. This functional dependence is shown in Tables 3 and 4. Interestingly, the stretch–bend coupling term is sensitive to the coordinate curvature; the magnitude of this term decreases as the coordinate curvature increases. Sibert and Colbert [18] found that minimizing this term as a function of the coordinate curvature was a useful way to predict which curvature leads to the most separable wave functions as based on the natural modal analysis. Here the central idea is that upon expanding the Hamiltonian one finds that there are both potential and kinetic contributions to k_{122}. The relative sizes of these contributions are a function of the coordinate curvature. In the rectilinear limit, the kinetic contribution is zero and the potential contribution for both SO_2 and H_2O is a maximum. As the curvature increases, the kinetic contribution to k_{122} increases and the potential contribution decreases. For both H_2O and SO_2 when $l \leqslant 0$ Å the two contributions lead to the smallest value of k_{122}. Since, in the perturbative treatment only the k_{122} terms leads to configuration interaction, this result is entirely consistent with the results of the maximum overlap criterion.

Using a Hamiltonian of this form, Baggott [51] fit the energy levels of H_2O and D_2O. An important goal of such fits is to provide insight into the nature of the underlying Born–Oppenheimer potential energy surface. The above constants, in conjunction with rotation–vibration interaction terms, provide, at least in principle, a quartic normal coordinate force field [47]. However, having obtained the coefficients from a fit to an experimental spectrum, one cannot know *a priori* which value of the curvature to use when inverting the spectrum. For example, the k_{122} coupling term is a measure of the stretch–bend coupling. If one compares the results of Baggott's [51] spectroscopic determination of k_{122} (cf. Table 4) to the value of this coefficient obtained from the perturbative expansion based on

Table 4. Spectroscopic constants for H_2O at various curvature values

Term	Rectilinear	Internal	Hypercurvature[a]	Ref. [51]
ω_1	3825.85	3825.85	3825.85	3829.02
ω_2	1650.66	1650.66	1650.66	1651.72
ω_3	3936.38	3936.38	3936.38	3942.04
χ_{11}	− 40.47	− 40.47	− 40.47	− 41.47
χ_{22}	− 13.60	− 17.13	− 17.86	− 18.91
χ_{33}	− 46.44	− 46.44	− 46.44	− 47.51
χ_{12}	− 33.43	− 19.32	− 16.40	− 19.20
χ_{13}	− 156.85	− 156.85	− 156.85	− 162.16
χ_{23}	− 19.61	− 19.61	− 19.61	− 19.04
$\lvert k_{122}\rvert$	133.98	56.06	9.07	37.57
k_{1133}	− 155.88	− 155.88	− 155.91	− 153.63

[a] $l = -0.35$ Å

rectilinear coordinates, one might argue that the force field of Halonen and Carrington [30] dramatically overestimates the amount of stretch-bend coupling. The results of Table 4 provide a clear demonstration of the dangers of such reasoning.

5. Concluding remarks

We have investigated the accuracy of independent mode descriptions for molecular vibrations as a function of a class of coordinates. In particular, we have quantified, for vibrational states of SO_2 and H_2O, the accuracy of independent mode models for determining: (1) eigenvalues using SCF and adiabatic energies and (2) eigenfunctions using natural modals and Brueckner functions. We have included in this study all those vibrational states whose excitation energies are less than 6100 cm^{-1} and less than 18 600 cm^{-1} for SO_2 and H_2O, respectively. The coordinates, the VCC, are a set of normal mode coordinates for which the curvature of the coordinate system is determined by a single parameter.

We found that the Brueckner functions and natural modals were nearly equivalent. For Brueckner functions, we showed that the curvature of the coordinate system that gives the maximum overlap with the exact eigenfunctions is greater than that of the curvilinear normal coordinates. In contrast, according to the best energy criterion, i.e. the least SCF energy, the rectilinear normal modes give the best description for the independent mode model. These results are surprising to the extent that, if the wave functions were indeed separable for some value of the coordinate curvature, then as one approached this value of the curvature, the SCF energy would approach the exact energy, and the overlap of the exact eigenfunction with the Brueckner function would approach unity. The adiabatic energies, which exploit a different dynamic separability, follow the similar trends as were observed for the SCF results. This work clearly elucidates the importance of examining several criteria simultaneously when looking for optimal sets of coordinates.

The coefficients of the spectroscopic Hamiltonian were investigated as a function of the curvature of the coordinate system. If the spectroscopic Hamiltonian

contains no off-diagonal coupling terms, then the eigenfunctions have the same form as an independent mode model. In contrast to the above independent mode results, the coefficients of the spectroscopic Hamiltonian are not a function of the coordinate curvature. On the other hand, if there are off-diagonal coupling terms, then the expansion coefficients are a function of the curvature. Using this result we highlighted the subtleties involved in extracting from a second order perturbative expansion the coefficients of a potential energy expansion.

Acknowledgements. We would like to thank D. T. Colbert for many useful discussions on using natural modals to examine vibrational wave functions and for useful enlightening commments on separability. This work was supported by National Science Foundation Grant No. CHE-9013904 and CHE-895764. The calculations were carried out using the Department of Chemistry Computer Center Facilities, partially supported by the National Science Foundation Grant No. CHE-9007850.

References

1. Carney GD, Sprandel LL, Kern CW (1978) Adv Chem Phys. 37:305
2. Sibert EL (1990) Int Rev Phys Chem 9:1
3. Sutcliffe BT, Tennyson J (1991) Int J Quant Chem 39:183
4. Handy NC (1989) Int Revs in Phys Chem 8:275
5. (1988) Comput Phys Commun 51 A thematic issue on molecular vibrations
6. Bačić Z, Light JC (1989) Annu Rev Phys Chem 40:469
7. Bramley MJ, Tromp JW, Carrington T Jr, Corey GC (1994) J Chem Phys 100:6175
8. Thompson TC, Truhlar DG (1982) J Chem Phys 77:3031
9. Moiseyev N (1983) Chem Phys Lett 98:233
10. Bačić Z, Gerber RB, Ratner MA (1986) J Phys Chem 90:3606
11. Zúñiga J, Bastida A, Requena A (1992) J Phys Chem 96:9691
12. Gibson LL, Roth RM, Ratner MA (1986) J Chem Phys 85:3425
13. Roth RM, Gerber RB, Ratner MA (1983) J Phys Chem 87:2376
14. Holmer BK, Certain PR (1985) J Phys Chem 89:4464
15. Moiseyev N, Schatzberger R, Froelich P, Goscinski O (1985) J Chem Phys 83:3924
16. Sage ML, Williams JA III (1983) J Chem Phys 78:1348
17. Stratt RM, Handy NC, Miller WH (1979) J Chem Phys 71:3311
18. Colbert DT, Sibert EL (1989) J Chem Phys 91:350
19. Fleming PR, Hutchinson JS (1989) J Chem Phys 90:1735
20. Kutzelnigg W, Smith VH, Jr (1964) J Chem Phys 41:896
21. Natanson GA, Ezra GS, Delgado-Barrio G, Berry RS (1984) J Chem Phys 81:3400
22. Johnson BR, Reinhardt WP (1986) J Chem Phys 85:4538
23. Romanowski H, Bowman JM (1984) Chem Phys Lett 110:235
24. Stefański K, Taylor HS (1985) Phys Rev A 31:2810
25. McCoy AB, Sibert EL (1991) J Chem Phys 95:3476
26. Wison EB, Decius JC, Cross PC (1955) Molecular vibrations, McGraw-Hill, New York
27. Bastida A, Requena A, Zúñiga J (1993) J Phys Chem 97:5831
28. Ratner MA, Gerber RB, Horn TR, Williams CJ (1991) In: Bowman JM (ed) Advances in molecular vibrations and collision dynamics, JAI Press Inc., Greenwich CT, p 215
29. Carter S, Mills IM, Murrell JN, Varandas AJC (1982) Mol Phys 45:1053
30. Halonen L, Carrington T, Jr (1988) J Chem Phys 88:4171
31. Carter C, Handy NC (1987) J Chem Phys 87:4294
32. Bačić Z, Light JC (1987) J Chem Phys 87:4008
33. Hamilton IP, Light JC (1986) J Chem Phys 84:306
34. Nesbet RK (1633) Phys Rev 109:1632; Primas H (1965) In: Sinanoglu O (ed) Modern quantum chemistry Part II, Academic, New York, p 45
35. Davidson ER (1976) Reduced density matrices in quantum chemsitry, Academic, New York.

36. Schwenke DW (1992) J Chem Phys 96:3426
37. Carlson BC, Keller JM (1961) Phys Rev 121:659
38. Löwdin PO, Shull H (1956) Phys Rev 101:1730
39. Gerber RB, Ratner MA (1988) Adv Chem Phys 70:97
40. Cooley JW (1961) Math Comp 15:363
41. Roothan CCJ (1951) Rev Mod Phys 23:69
42. Hose G, Taylor H, Bai YY (1984) J Chem Phys 80:4363
43. Certain PR, Moiseyev N (1987) J Chem Phys 86:2146
44. Baggott JE (1987) Mol Phys 62:1019
45. McCoy AB, Sibert EL (1990) J Chem Phys 92:1893
46. Kauppi E, Halonen L (1992) J Chem Phys 96:2933
47. Mills IM (1972) In: Rao KN, Mathews CW (eds) Molecular spectroscopy: modern research, Academic Press, New York.
48. Dennison DM (1940) Rev Mod Phys 12:175
49. Nielsen HH (1951) Rev Mod Phys 23:90
50. Benedict WS, Gailar N, Plyler EK (1956) J Chem Phys 24:139
51. Baggott JE (1988) Mol Phys 65:739